INSTITUTE OF PHYSICS PUBLISHING JOURNAL OF PHYSICS A: MATHEMATICAL AND GENERAL

J. Phys. A: Math. Gen. **34** (2001) 10029–10043 PII: S0305-4470(01)25097-5

Alignment indices: a new, simple method for determining the ordered or chaotic nature of orbits

Ch Skokos

Research Center for Astronomy, Academy of Athens, 14 Anagnostopoulou street, GR-106 73, Athens, Greece

E-mail: hskokos@cc.uoa.gr

Received 17 May 2001, in final form 3 August 2001
Published 16 November 2001
Online at stacks.iop.org/JPhysA/34/10029

Abstract

We introduce a new, simple and efficient method for determining the ordered or chaotic nature of orbits in two-dimensional (2D), four-dimensional (4D) and six-dimensional (6D) symplectic maps: the computation of the alignment indices. For a given orbit we follow the evolution in time of two different initial deviation vectors computing the norms of the difference d_- (parallel alignment index) and the addition d_+ (antiparallel alignment index) of the two vectors. The time evolution of the smaller alignment index reflects the chaotic or ordered nature of the orbit. In 2D maps the smaller alignment index tends to zero for both ordered and chaotic orbits but with completely different time rates, which allows us to distinguish between the two cases. In 4D and 6D maps the smaller alignment index tends to zero in the case of chaotic orbits, while it tends to a positive non-zero value in the case of ordered orbits. The efficiency of the new method is also shown in a case of weak chaos and a comparison with other known methods that separate chaotic from regular orbits is presented.

PACS numbers: 05.45.−a, 05.45.Jn, 05.45.Ac

1. Introduction

The problem of distinguishing between ordered and chaotic motion in a dynamical system, especially one with many degrees of freedom, is fundamental in a large area of modern science. Thus we need fast and accurate tools to give us information about the chaotic or ordered character of an orbit, mainly when the dynamical system has many degrees of freedom (at least three) because then it is not easy to inspect the phase space.

Some well-known methods that try to give an answer to this problem are as follows:

(a) The inspection of the consequents of an orbit on a Poincaré surface of section. For 2D systems this method has been used extensively, despite the problem of finding a proper

Poincaré surface of section. However, the inspection becomes very difficult and greatly deceiving for systems with multidimensional phase space.

(b) The maximal Lyapunov characteristic number (LCN) of an orbit informs us whether an orbit is ordered or chaotic. The LCN is the limit of the finite time Lyapunov characteristic number

$$L_t = \frac{1}{t} \ln \frac{|\xi_t|}{|\xi_0|} \tag{1}$$

(where ξ_0 and ξ_t are the distances between two points of two nearby orbits at times $t = 0$ and t), when t tends to infinity. In other words, LCN gives the average exponential deviation of two nearby orbits, so if LCN $= 0$ the orbit is ordered and if LCN > 0 the orbit is chaotic. In mappings t is discrete time, i.e. the number N of iterations of the map, so the finite time Lyapunov characteristic number can be denoted as L_N. An advantage of this method is that it can be applied to systems of any number of degrees of freedom.

(c) The frequency analysis method of Laskar [1–5], based on calculating the basic frequencies of an orbit over a fixed interval of time. For orbits on KAM tori these frequencies are very accurate approximations of the actual frequencies of the system but for chaotic orbits the computed values vary significantly in time and space. This method can be applied to systems with many degrees of freedom.

In recent years the following new techniques have been developed:

(i) The study of spectra of 'short time Lyapunov characteristic numbers' [6, 7] or 'stretching numbers' α [8–10], and the spectra of helicity angles Φ and twist angles ϕ [11–13]. The stretching number α is the logarithm of the ratio of two successive deviations $|\xi_{t+\Delta t}|$ and $|\xi_t|$ at times differing by Δt. In mappings the smallest value of Δt is 1 so the stretching number is

$$\alpha_i = \ln \frac{|\xi_{i+1}|}{|\xi_i|} \tag{2}$$

where i counts the iterations of the mapping. The helicity angle is the angle between a deviation vector ξ_i with a fixed direction (say the axis x_1) and the twist angle is the difference of two successive helicity angles. In a phase space of more than two dimensions $(x_1, x_1, \ldots, x_n)$ we project ξ_i on the planes $(x_2, x_1), (x_3, x_1), \ldots, (x_n, x_1)$ and take the angles Φ_i and ϕ_i on all these planes ($i = 1, 2, \ldots, n-1$).

If Q is one of these quantities, i.e. $Q = \alpha, \Phi, \phi$, we define the 'dynamical spectrum of Q', i.e. the probability density of the values of Q given by

$$S(Q) = \frac{dN(Q, Q + \mathrm{d}Q)}{N \cdot \mathrm{d}Q} \tag{3}$$

where N is the total number of iterations and $\mathrm{d}N(Q, Q + \mathrm{d}Q)$ is the number of values of Q in the interval (bin) $(Q, Q + \mathrm{d}Q)$.

For Hamiltonian systems with two degrees of freedom, or equivalently for 2D maps, the spectra of stretching numbers, helicity and twist angles have been used successfully in distinguishing between ordered and chaotic orbits [10, 12, 13]. In multidimensional systems we have a plethora of angular dynamical spectra. On the other hand, the stretching number is independent of the dimension of the phase space, so its spectra can be used easily for the determination of the ordered or chaotic nature of an orbit.

In a recent paper by Voglis *et al* [14] a new numerical quantity was introduced for determining whether an orbit is ordered or chaotic in 4D maps. This quantity is the

'spectral distance' D between two spectra $S_1(\alpha)$ and $S_2(\alpha)$ produced for the same orbit but with different initial deviation vectors

$$D^2 = \sum_{\text{all } \alpha} [S_1(\alpha) - S_2(\alpha)]^2 \cdot \mathrm{d}\alpha \tag{4}$$

where $\mathrm{d}\alpha$ is the constant width of the bin of stretching numbers. One of the main conclusions of that paper is that when the motion is ordered, the spectra produced by two different initial deviation vectors are different, so D tends to a constant non-zero value, while for chaotic motion the final spectra will be equal and D tends to zero.

(ii) The fast Lyapunov indicator (FLI) [15, 16]. The FLI is defined as follows. In an n-dimensional phase space we take an n-dimensional vector basis $V_n(0) = (v_1(0), v_2(0), \ldots, v_n(0))$ as n initial deviation vectors from an orbit with initial condition $P(0) = (x_1(0),\ x_2(0), \ldots, x_n(0))$. Then we evolve the deviation vectors and the orbit in time and at every time step (for Hamiltonian systems) or iteration (for maps) we take the largest among the vectors of the evolving basis and define FLI as

$$\mathrm{FLI} = \sup_j \|v_j(t)\| \qquad j = 1, 2, \ldots, n. \tag{5}$$

For both ordered and chaotic orbits FLI tends to infinity as time t, or the number N of iterations, increases, following however completely different time rates which allows us to distinguish between the two cases.

In the present paper we introduce a new, fast and easy to compute indicator of the chaotic or ordered nature of orbits: the alignment indices (ALIs). The paper is organized as follows. In section 2 we define the parallel and antiparallel alignment indices explaining the different behaviour they exhibit for ordered and chaotic orbits. In section 3 we apply the method of the alignment indices to ordered and chaotic orbits of a 2D map (section 3.1), of a 4D map (section 3.2) and of a 6D map (section 3.3), giving a comparison with other methods and in particular with (a) inspection of the consequents of orbits on the Poincaré surface of section of the system, (b) the finite time Lyapunov characteristic number L_N, (c) the FLI and (d) the spectral distance D between the spectra of stretching numbers produced by two different deviation vectors. The efficiency of the ALIs is shown in a case of weak chaos studied in section 4. Finally in section 5 we summarize our results and present our conclusions. We note that all the maps considered in the present paper are symplectic maps, so they represent conservative dynamical systems.

2. Definition of the alignment indices

It is known that the spectra of stretching numbers in 2D maps are invariant with respect to the choice of the initial deviation vector for ordered and chaotic orbits [8]. The case of 4D maps is quite different. In 4D maps the ordered motion occurs on a 2D torus. Any initial deviation vector becomes almost tangent to this torus after a short transient period. In general, two different initial deviation vectors become tangent to different directions on the torus producing different sequences of vectors and hence different spectra. On the other hand, in chaotic cases two initially different deviation vectors tend to coincide with the direction defined by the most unstable nearby manifold and hence coincide with each other, or one vector tends to the opposite of the other producing equal spectra of stretching numbers. So the spectral distance D (4) of the two spectra tends to zero for chaotic orbits and to a constant non-zero value for ordered orbits [14]. Discussion on the theoretical approach of the behaviour of the deviation vectors in 2D and 4D maps can be found in [17].

Instead of following the evolution of the spectra of stretching numbers produced by two different initial deviation vectors (e.g. $v_1(0)$, $v_2(0)$) and the corresponding spectral distance D, we can decide if an orbit is ordered or chaotic by following the evolution in time of the two deviation vectors. We define as the parallel alignment index, the quantity

$$d_- \equiv \|v_1(t) - v_2(t)\| \tag{6}$$

and as the antiparallel alignment index, the quantity

$$d_+ \equiv \|v_1(t) + v_2(t)\| \tag{7}$$

where $\|\cdot\|$ denotes the Euclidean norm of a vector. It is obvious from the above definitions that when $d_- = 0$ the two vectors coincide and when $d_+ = 0$ the two vectors are opposite.

If we consider the vectors v_1 and v_2 to be normalized with norm equal to 1, the two deviation vectors of a chaotic orbit tend to coincide when $d_- \to 0$ and $d_+ \to 2$ and tend to become opposite when $d_- \to 2$ and $d_+ \to 0$. If the orbit is ordered, the two vectors become tangent to the torus on which the orbit is confined, in different directions. Then both quantities d_+ and d_- tend to positive values in the interval $(0, 2)$. So, the smaller alignment index (SALI) tends to zero when the orbit is chaotic and to a non-zero value when the orbit is ordered. The different behaviour of SALI for ordered and chaotic orbits, makes it a good, easy to compute and very fast (as shown further on) tool in order to define the ordered or chaotic nature of an orbit in n-dimensional maps with $n \geqslant 4$.

In 2D maps the two deviation vectors tend to coincide or become opposite for ordered and chaotic orbits. The ordered motion occurs on a 1D torus, the so-called invariant curve. So, any two deviation vectors eventually become tangent to this curve, tending to coincide or become opposite to each other. For chaotic orbits we have a similar case since any two deviation vectors become tangent to the most unstable nearby manifold. As a consequence, the spectra of stretching numbers tend to coincide in both cases. Thus, the spectral distance D tends to zero in both cases, so it cannot distinguish between ordered and chaotic motion. On the other hand, although one of the ALIs d_-, d_+ and the SALI tend to zero, both in ordered and chaotic cases, they follow completely different time rates for ordered and chaotic orbits (as shown in section 3.1) and this allows us to distinguish between the two cases.

3. Application of the alignment indices

The dynamical systems we use to demonstrate the method of ALIs are simple symplectic maps with two, four and six dimensions. In particular we use the 2D map

$$\begin{aligned} x_1' &= x_1 + x_2 \\ x_2' &= x_2 - \nu \sin(x_1 + x_2) \end{aligned} \qquad (\text{mod } 2\pi) \tag{8}$$

and the 4D map

$$\begin{aligned} x_1' &= x_1 + x_2 \\ x_2' &= x_2 - \nu \sin(x_1 + x_2) - \mu[1 - \cos(x_1 + x_2 + x_3 + x_4)] \\ x_3' &= x_3 + x_4 \\ x_4' &= x_4 - \kappa \sin(x_3 + x_4) - \mu[1 - \cos(x_1 + x_2 + x_3 + x_4)] \end{aligned} \qquad (\text{mod } 2\pi) \tag{9}$$

which is composed of two 2D maps of the form (8), with parameters ν and κ, coupled with a term of the order μ. All variables are given (mod 2π), so $x_i \in [-\pi, \pi)$, for $i = 1, 2, 3, 4$. The map (9) is a variant of Froeschlé's 4D symplectic map [18]. The periodic orbits of map (9) and their bifurcations have been studied by Contopoulos and Giorgilli [19]. Structures in the phase space of this map for small values of the coupling parameter μ were examined in detail by Skokos *et al* [20].

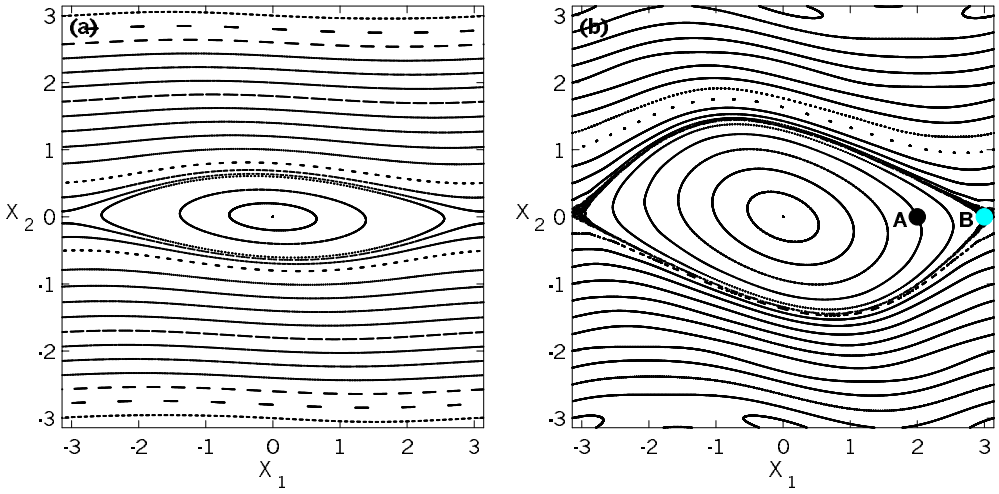

Figure 1. Phase plots of the 2D map (8) for (*a*) $\nu = 0.1$ and (*b*) $\nu = 0.5$. In (*b*) the initial conditions of the ordered orbit A ($x_1 = 2,\ x_2 = 0$) and the chaotic orbit B ($x_1 = 3,\ x_2 = 0$) are marked by black and light-grey full circles, respectively.

The 6D map we use

$$\begin{aligned}
x_1' &= x_1 + x_2' \\
x_2' &= x_2 + \frac{K}{2\pi}\sin(2\pi x_1) - \frac{\beta}{2\pi}\{\sin[2\pi(x_5 - x_1)] + \sin[2\pi(x_3 - x_1)]\} \\
x_3' &= x_3 + x_4' \\
x_4' &= x_4 + \frac{K}{2\pi}\sin(2\pi x_3) - \frac{\beta}{2\pi}\{\sin[2\pi(x_1 - x_3)] + \sin[2\pi(x_5 - x_3)]\} \qquad (\text{mod } 1) \qquad (10) \\
x_5' &= x_5 + x_6' \\
x_6' &= x_6 + \frac{K}{2\pi}\sin(2\pi x_5) - \frac{\beta}{2\pi}\{\sin[2\pi(x_3 - x_5)] + \sin[2\pi(x_1 - x_5)]\}
\end{aligned}$$

is composed of three coupled standard maps. The map (10) is the $n = 3$ case of the n-coupled standard maps studied by Kantz and Grassberger [21]. All variables are given (mod 1), so $x_i \in [0, 1)$, for $i = 1, 2, \ldots, 6$. For $\beta = 0$ map (10) gives three uncoupled standard maps. For $\beta \neq 0$ the maps are coupled and influence each other.

3.1. Ordered and chaotic orbits in a 2D map

First we study ordered and chaotic orbits in the 2D map (8). For $\nu = 0$ the map (8) is reduced to two independent 1D maps, where x_2 is constant. When the constant $x_2 = -2\pi m/n$, (mod 2π) with $m, n \in N^*$ and $m \leqslant n$, on the plane x_1x_2 we have n points, and any two successive consequents are located m points apart. So the map (8) on the plane x_1x_2 consists of points on lines parallel to the axis $x_2 = 0$, or of horizontal rows of n points. By setting $\nu = 0.1$ we have a 2D map with a small coupling so the picture we take does not differ much from that with $\nu = 0$. The difference is in the region near the stable periodic orbit $x_1 = x_2 = 0$, where we no longer have horizontal lines, but closed curves (figure 1(*a*)). For $\nu = 0.5$, the central island around the origin $x_1 = x_2 = 0$ is larger and a small chaotic region around the unstable periodic orbit $x_1 = -\pi,\ x_2 = 0$ is visible (figure 1(*b*)).

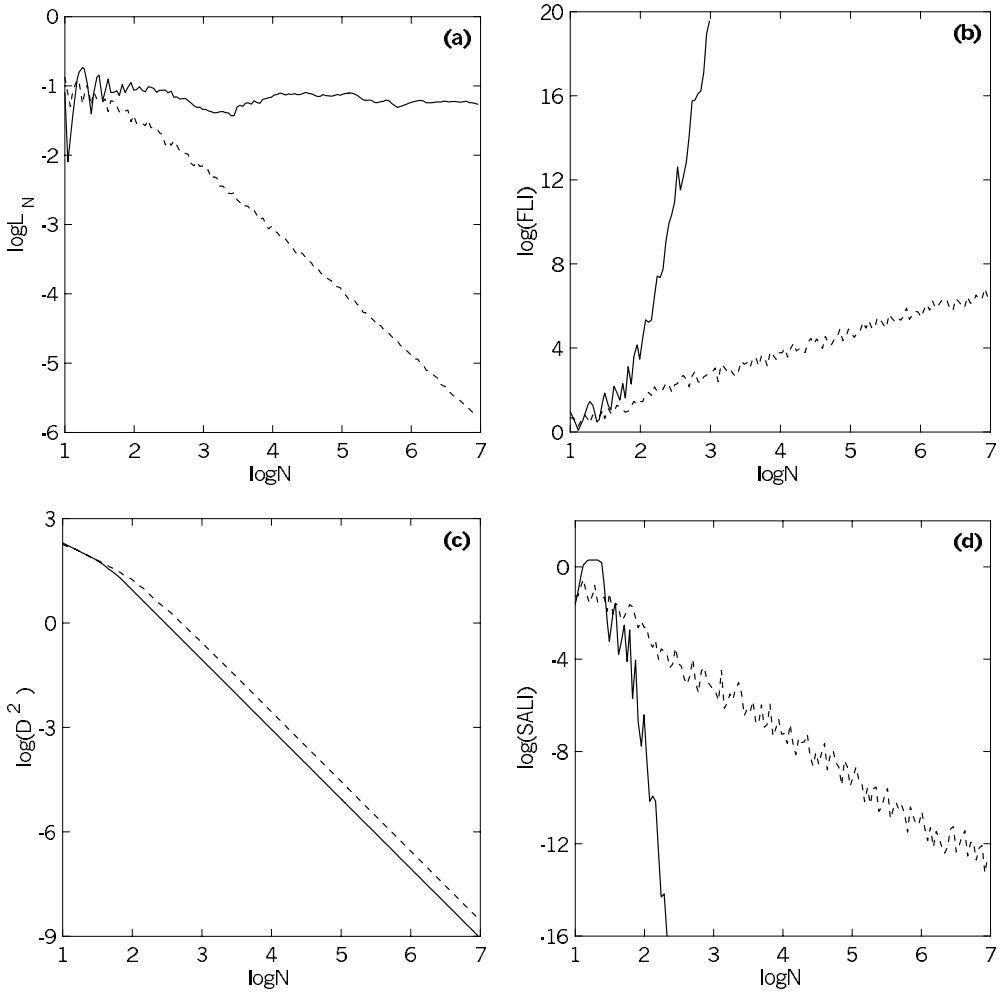

Figure 2. The evolution of (*a*) the finite time Lyapunov characteristic number L_N, (*b*) the fast Lyapunov indicator FLI, (*c*) the square of the spectral distance D and (*d*) the smaller alignment index SALI, with respect to the number N of iterations of the 2D map (8) with $\nu = 0.5$, for the ordered orbit A with initial conditions $x_1 = 2,\ x_2 = 0$ (dashed curves) and for the chaotic orbit B with initial conditions $x_1 = 3,\ x_2 = 0$ (solid curves).

We consider for our study the ordered orbit A with initial conditions $x_1 = 2,\ x_2 = 0$ and the chaotic orbit B with initial conditions $x_1 = 3,\ x_2 = 0$ of the 2D map (8) with $\nu = 0.5$. The initial conditions of these orbits are marked in figure 1(*b*).

The evolution of the finite time Lyapunov characteristic number L_N for both orbits is shown in figure 2(*a*). As expected for ordered orbits, L_N of orbit A (dashed curve) decreases as the number N of iterations increases, following a power law, reaching the value $L_N \approx 1.6 \times 10^{-6}$ after 10^7 iterations. On the other hand L_N of the chaotic orbit B (solid curve), after some fluctuations seems to stabilize near a constant value and it becomes $L_N \approx 5 \times 10^{-2}$ after 10^7 iterations.

For both orbits we compute the FLIs (5) using the initial deviation vectors (1, 0) and (0, 1). The results are shown in figure 2(*b*). The FLI of the ordered orbit A increases as N

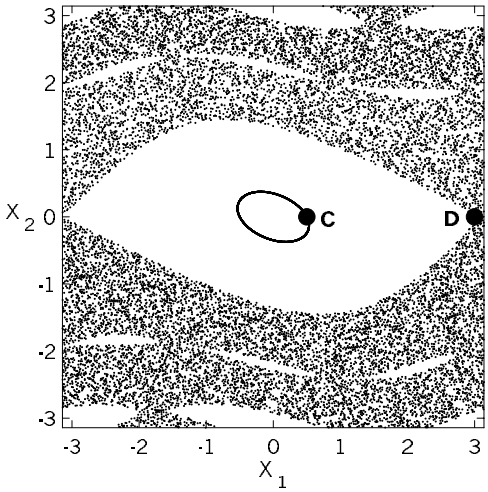

Figure 3. Projections of the orbits of the 4D map (9) for $\nu = 0.5$, $\kappa = 0.1$, $\mu = 10^{-3}$, with initial conditions $x_1 = 0.5$, $x_2 = 0$, $x_3 = 0.5$, $x_4 = 0$ (ordered orbit C) and $x_1 = 3$, $x_2 = 0$, $x_3 = 0.5$, $x_4 = 0$ (chaotic orbit D) on the x_1x_2 plane. The initial conditions of the orbits are marked by full circles.

increases following a power law (dashed curve). In the case of the chaotic orbit B the FLI increases abruptly reaching the value 10^{20} after about 1000 iterations (solid curve).

Since the map (8) is two-dimensional two deviation vectors tend to coincide or become opposite, producing equal spectra of stretching numbers. So, the spectral distance D tends to zero, both for ordered and chaotic orbits. In figure 2(c) we see the evolution of the spectral distance D of the spectra of stretching numbers produced by the initial deviation vectors (1, 0) and (0, 1), for the ordered orbit A (dashed curve) and the chaotic orbit B (solid curve). In both cases D decreases following the same power law. It is evident that D cannot be used to separate between ordered and chaotic motion in 2D maps.

The deviation vectors eventually coincide or become opposite for ordered and chaotic orbits, but on completely different time rates. This is evident from figure 2(d), where the smaller alignment index (SALI) is plotted as a function of the number N of iterations, both for the ordered orbit A (dashed curve) and the chaotic orbit B (solid curve). The initial deviation vectors used are (1, 0) and (0, 1). The SALI is the parallel alignment index d_- in both cases, which means that the two deviation vectors tend to coincide.

For the ordered orbit A the SALI decreases as N increases, following a power law and it becomes SALI $\approx 10^{-13}$ after 10^7 iterations, which means that the two deviation vectors almost coincide. The SALI of the chaotic orbit B decreases abruptly, reaching the limit of accuracy of the computer (10^{-16}) after about 200 iterations. After that time the two vectors are identical since their coordinates are represented by the same numbers in the computer. So, the SALI can distinguish between ordered and chaotic motion on a 2D map, since it decreases to zero following completely different time rates.

3.2. Ordered and chaotic orbits in a 4D map

Now we consider the case of the 4D map (9) for $\nu = 0.5$, $\kappa = 0.1$ and $\mu = 10^{-3}$. So, we have a weak coupling of the 2D map (8) for $\nu = 0.5$ on the plane x_1x_2 shown in figure 1(b), with the 2D map (8) for $\nu = 0.1$ on the plane x_3x_4 shown in figure 1(a). We consider the orbit C with initial conditions $x_1 = 0.5$, $x_2 = 0$, $x_3 = 0.5$, $x_4 = 0$ and the orbit D with initial conditions

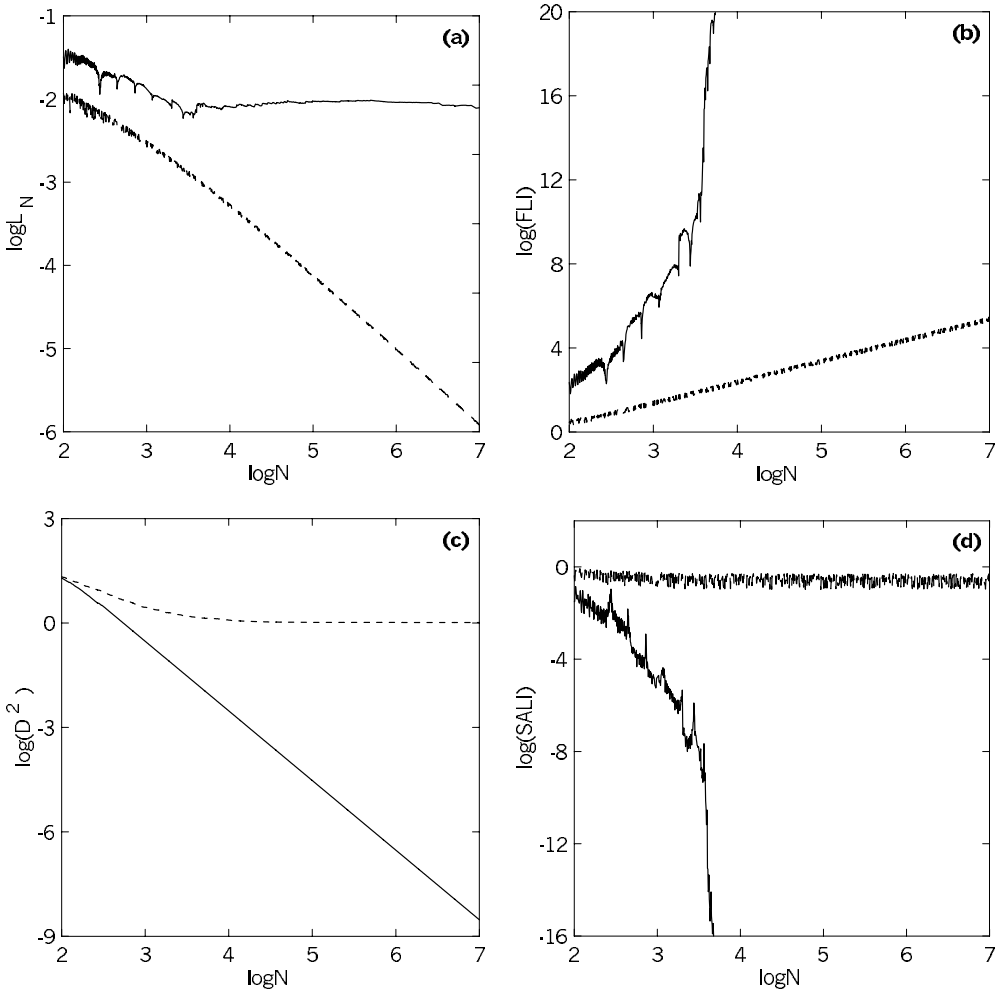

Figure 4. The evolution of (*a*) L_N, (*b*) FLI, (*c*) D^2 and (*d*) SALI, with respect to the number N of iterations of the 4D map (9) with $\nu = 0.5$, $\kappa = 0.1$, $\mu = 10^{-3}$, for the ordered orbit C with initial conditions $x_1 = 0.5$, $x_2 = 0$, $x_3 = 0.5$, $x_4 = 0$ (dashed curves) and for the chaotic orbit D with initial conditions $x_1 = 3$, $x_2 = 0$, $x_3 = 0.5$, $x_4 = 0$ (solid curves).

$x_1 = 3$, $x_2 = 0$, $x_3 = 0.5$, $x_4 = 0$. The projections on the x_1x_2 plane of some thousands of consequents of these orbits, as well as their initial conditions, are shown in figure 3. We can predict that orbit C is ordered, since its projection on the x_1x_2 plane forms a closed curve, while orbit D is chaotic, since it produces scattered points on the x_1x_2 plane.

In order to define the nature of orbits C and D we compute the same quantities as in the case of the 2D map (8). From the evolution of L_N, shown in figure 4(a), we see that orbit C is ordered, since L_N decreases with respect to N following a power law and becoming $L_N \approx 10^{-6}$ after 10^7 iterations (dashed curve). Orbit D is chaotic, since L_N stabilizes after about 10^4 iterations and it becomes $L_N \approx 8 \times 10^{-3}$ after 10^7 iterations (solid curve).

The FLIs of both orbits are computed by using the initial deviation vectors (1, 1, 1, 1), (1, 0, 0, 0), (0, 1, 0, 0) and (0, 0, 1, 0), and plotted in figure 4(*b*). The FLI of orbit C (dashed curve) increases as N increases following a power law, while the FLI of orbit D (solid curve) increases abruptly reaching the value 10^{20} after about 5.5×10^3 iterations.

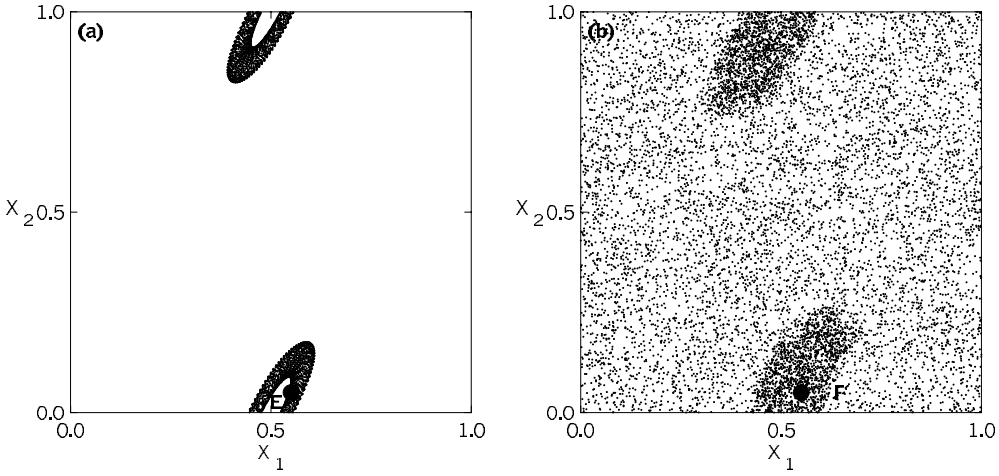

Figure 5. Projections on the x_1x_2 plane of the orbits of the 6D map (10) for $K = 3$, $\beta = 0.1$, with initial conditions (*a*) $x_1 = 0.55$, $x_2 = 0.05$, $x_3 = 0.55$, $x_4 = 0.01$, $x_5 = 0.55$, $x_6 = 0$ (ordered orbit E) and (*b*) $x_1 = 0.55$, $x_2 = 0.05$, $x_3 = 0.55$, $x_4 = 0.21$, $x_5 = 0.55$, $x_6 = 0$ (chaotic orbit F). The initial conditions of the orbits are marked by full circles.

In figure 4(*c*) we see the evolution of D of the spectra of stretching numbers produced by the initial deviation vectors (1, 1, 1, 1) and (1, 0, 0, 0) for the ordered orbit C (dashed curve) and the chaotic orbit D (solid curve). In the case of the ordered orbit C the spectral distance D starts to stabilize to a non-zero value after about 10^4 iterations, while in the case of the chaotic orbit D it decreases as N increases and tends to zero following a power law.

In figure 4(*d*) the SALI is plotted with respect to the number N of iterations of the 4D map (9) for the orbits C (dashed curve) and D (solid curve). The initial deviation vectors used are (1, 1, 1, 1) and (1, 0, 0, 0). In particular the SALI is the parallel alignment index d_- for orbit C, while it is the antiparallel alignment index d_+ for orbit D. That means that the two deviation vectors become opposite in the case of the chaotic orbit D. For the ordered orbit C the SALI remains almost constant, fluctuating around SALI ≈ 0.28, while it decreases abruptly in the case of the chaotic orbit D, reaching the limit of accuracy of the computer (10^{-16}) after about 4.7×10^3 iterations. After that time the coordinates of the two vectors are represented by opposite numbers in the computer.

3.3. Ordered and chaotic orbits in a 6D map

As a case of a multidimensional map we consider the 6D map (10). For $K = 3$ and $\beta = 0.1$ we consider the ordered orbit E with initial conditions $x_1 = 0.55$, $x_2 = 0.05$, $x_3 = 0.55$, $x_4 = 0.01$, $x_5 = 0.55$, $x_6 = 0$ and the chaotic orbit F with initial conditions $x_1 = 0.55$, $x_2 = 0.05$, $x_3 = 0.55$, $x_4 = 0.21$, $x_5 = 0.55$, $x_6 = 0$. Orbit E remains trapped in a finite region of the phase space, with its projections on the planes x_3x_4 and x_5x_6 being similar to the one on the plane x_1x_2, seen in figure 5(*a*). On the other hand, the orbit F initially stays in a region similar to the one occupied by orbit E, but after about 3000 iterations it spreads through the entire phase space, as seen in figure 5(*b*).

The evolution of L_N for orbits E (dashed curve) and F (solid curve) is shown in figure 6(*a*). From this figure we conclude that orbit E is ordered since L_N decreases with respect to N following a power law, reaching $L_N \approx 1.3 \times 10^{-6}$ after 10^7 iterations. Orbit F is chaotic

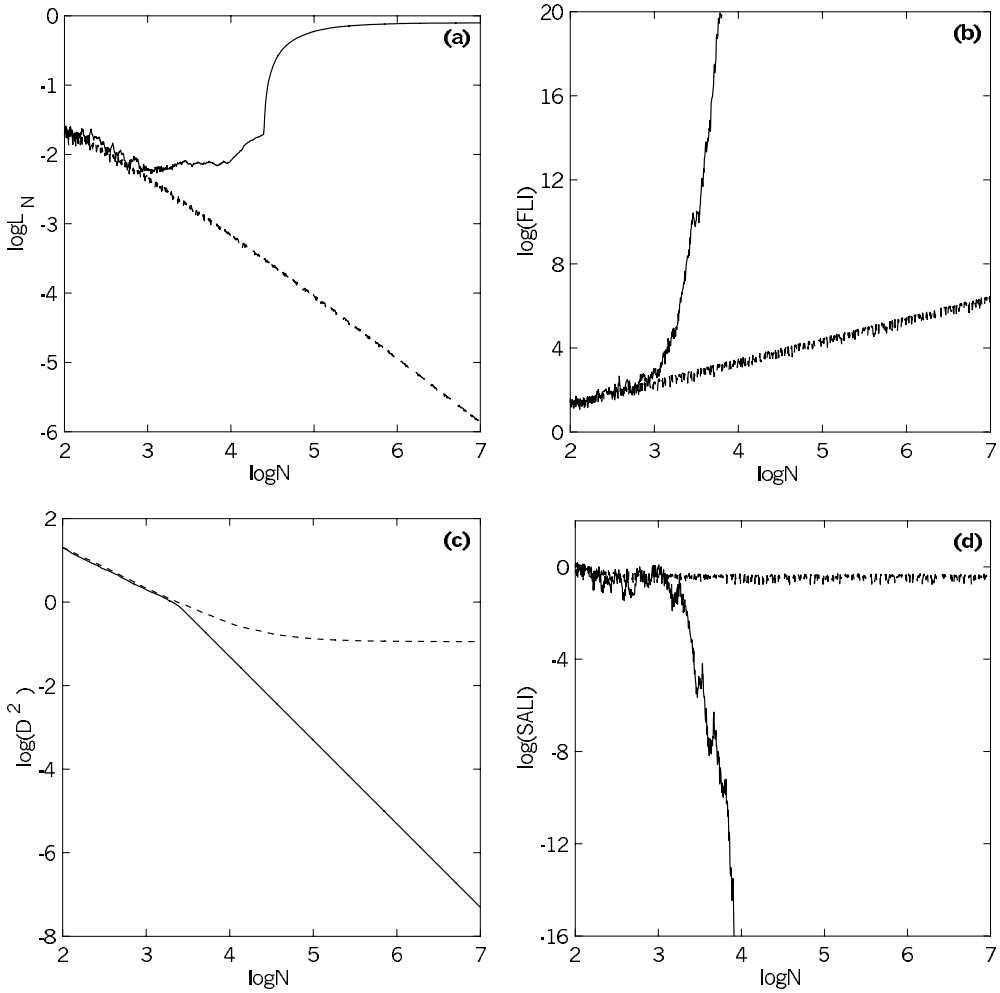

Figure 6. The evolution of (*a*) L_N, (*b*) FLI, (*c*) D^2 and (*d*) SALI, with respect to the number N of iterations of the 6D map (10) with $K = 3$, $\beta = 0.1$, for the ordered orbit E with initial conditions $x_1 = 0.55$, $x_2 = 0.05$, $x_3 = 0.55$, $x_4 = 0.01$, $x_5 = 0.55$, $x_6 = 0$ (dashed curves) and for the chaotic orbit F with initial conditions $x_1 = 0.55$, $x_2 = 0.05$, $x_3 = 0.55$, $x_4 = 0.21$, $x_5 = 0.55$, $x_6 = 0$ (solid curves).

since L_N does not tend to zero, but stabilizes after about 10^5 iterations near a constant non-zero value, becoming $L_N \approx 0.1$ after 10^7 iterations.

The FLIs of both orbits are computed by using the initial deviation vectors (1, 0, 0, 0, 0, 0), (0, 1, 0, 0, 0, 0), (0, 0, 1, 0, 0, 0), (0, 0, 0, 1, 0, 0), (0, 0, 0, 0, 1, 0), (0, 0, 0, 0, 0, 1) and plotted in figure 6(*b*). The FLI of the ordered orbit E increases as N increases, following a power law (dashed curve). The FLI of the chaotic orbit F increases abruptly after about 10^3 iterations reaching the value 10^{20} after about 6500 iterations (solid curve).

The spectral distance D of the spectra of stretching numbers produced by the initial deviation vectors (1, 0, 0, 0, 0, 0), (0, 1, 0, 0, 0, 0) is shown in figure 6(*c*) both for the ordered orbit E (dashed curve) and the chaotic orbit F (solid curve). After a transient phase D tends to a constant non-zero value for orbit E, while it tends to zero for orbit F, as expected.

In figure 6(*d*) the SALI is plotted with respect to the number N of iterations of the 6D map (10) for orbits E (dashed curve) and F (solid curve). The initial deviation vectors used are (1, 0, 0, 0, 0, 0), (0, 1, 0, 0, 0, 0). The SALI is the antiparallel alignment index d_+ in both cases, which means that the two deviation vectors become opposite in the case of the chaotic orbit F. The SALI remains almost constant for the ordered orbit E, fluctuating around SALI $\approx$ 0.4. In the case of the chaotic orbit F the SALI decreases abruptly after about 10^3 iterations, reaching the limit of accuracy of the computer (10^{-16}) after about 8×10^3 iterations.

It is evident from the above results that the behaviour of all the quantities shown in figure 6 is similar to that exhibited in the case of the 4D map studied in section 3.2.

We see that the SALI clearly distinguishes between ordered and chaotic motion in 4D maps (and also in n-dimensional maps with $n > 4$), because it fluctuates around a non-zero value for ordered orbits, while it decreases to zero for chaotic orbits.

4. A case of weak chaos

In order to test the efficiency of the SALI in distinguishing between ordered and chaotic motion we apply it to a known case of weak chaos [11, 14]. We use the model of two coupled standard maps

$$\begin{aligned} x_1' &= x_1 + x_2' \\ x_2' &= x_2 + \frac{K}{2\pi}\sin(2\pi x_1) - \frac{\beta}{\pi}\sin[2\pi(x_3 - x_1)] \\ x_3' &= x_3 + x_4' \\ x_4' &= x_4 + \frac{K}{2\pi}\sin(2\pi x_3) - \frac{\beta}{\pi}\sin[2\pi(x_1 - x_3)] \end{aligned} \quad (\text{mod } 1) \qquad (11)$$

For $K = 3$ we select two orbits with the same initial conditions, i.e. $x_1 = 0.55,\ x_2 = 0.1,\ x_3 = 0.62,\ x_4 = 0.2$ for $\beta = 0.1$ (orbit G) and $\beta = 0.3051$ (orbit H). As explained by Voglis *et al* [14], orbit G is ordered while orbit H is slightly chaotic having a very small LCN. The projections of 5×10^3 points of the orbits G and H after 10^7 iterations of the 4D map (11) on the planes x_1x_2 and x_3x_4, respectively, are shown in figures 7(*a*) and (*b*) for orbit G and in figures 7(*c*) and (*d*) for orbit H. The projections of both orbits fill similar regions in the phase space and give the impression of motion on a torus, leading us to consider wrongly that both orbits are ordered.

The evolution of L_N for both orbits is given in figure 8(*a*). The L_N of orbit G (dashed curve) decreases as N increases, following a power law and it becomes $L_N \approx 1.6 \times 10^{-7}$ after 10^8 iterations, denoting that orbit G is ordered. On the other hand the L_N of orbit H (solid curve) looks similar to orbit G up to 2×10^7 iterations, but beyond that we see a difference between the two curves. After 10^8 iterations L_N of orbit H stops decreasing but one has to wait up to 10^9 iterations in order to see it stabilized near a small but non-zero value ($L_N \approx 5 \times 10^{-7}$). This means that orbit H is slightly chaotic, but one has to wait at least up to 10^8 iterations in order to have an indication of its stochasticity and up to 10^9 iterations in order to be certain that the orbit is chaotic.

The FLIs of orbits G and H are computed using the initial deviation vectors (1, 1, 1, 1), (1, 2, 1, 2), (0, 0, 1, 0), (0, 0, 0, 1) and plotted in figure 8(*b*). Both curves evolve in a similar way up to 10^7 iterations. After that point the FLI of orbit H (solid curve) increases abruptly and becomes 10^{20} after about 8.2×10^7 iterations, while the FLI of orbit G (dashed curve) continues to increase following the same power law as before. So, after about 5×10^7 iterations one can be certain that orbit H is chaotic.

In figure 8(*c*) we see that, for both orbits, the spectral distance D between the spectra of stretching numbers produced by the initial deviation vectors (1, 1, 1, 1) and (1, 2, 1, 2),

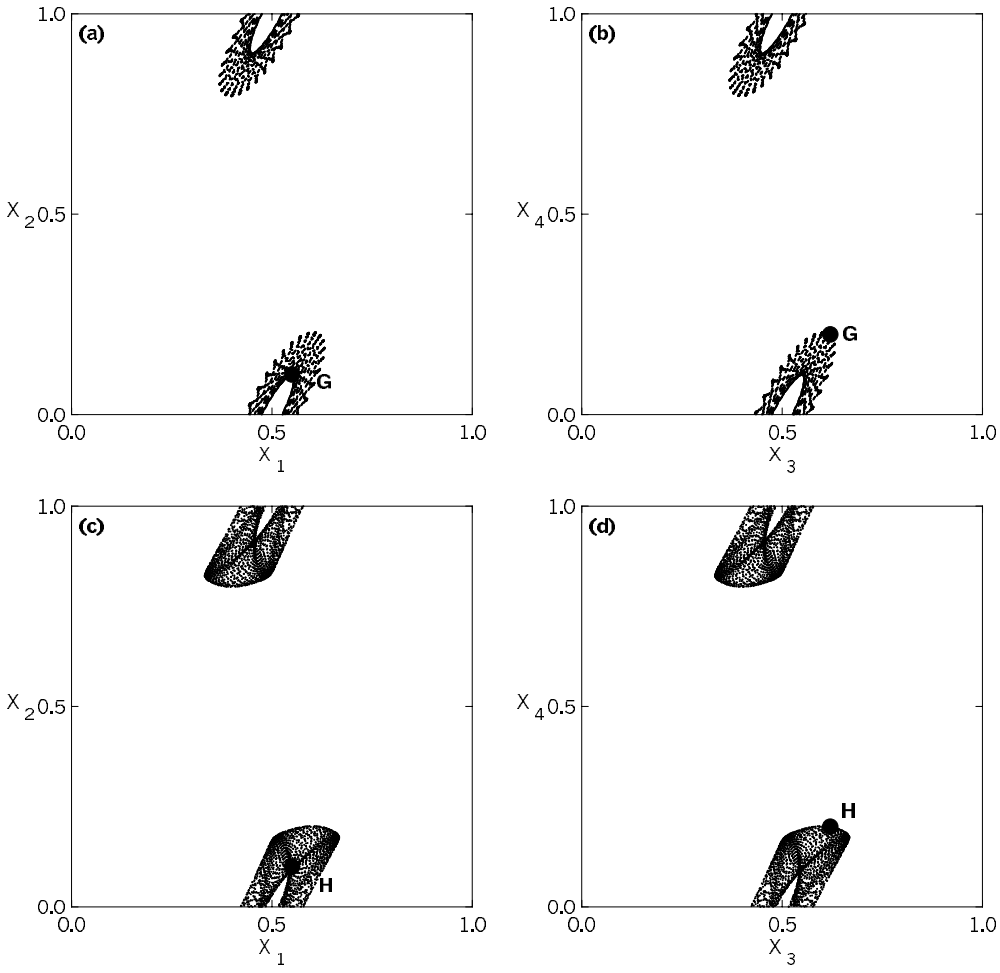

Figure 7. Projections of the orbits of the 4D map (11) with $K = 3$ and initial conditions $x_1 = 0.55$, $x_2 = 0.1$, $x_3 = 0.62$, $x_4 = 0.2$ for (i) $\beta = 0.1$s (ordered orbit G) on the planes (*a*) x_1x_2 and (*b*) x_3x_4 and for (ii) $\beta = 0.3051$ (slightly chaotic orbit H) on the planes (*c*) x_1x_2 and (*d*) x_3x_4. The initial conditions of the orbits are marked by filled circles.

decreases in a similar way up to 10^6 iterations. At that time the two curves separate, although they continue to decrease. The curve of orbit G (dashed curve) starts to stabilize around a non-zero value after about 10^7 iterations, while the curve of orbit H (solid curve) continues to decrease. After about 5×10^7 iterations the different behaviour of D for the two orbits is evident.

The evolution of the SALI for orbits G and H is shown in figure 8(*d*). The initial deviation vectors used for the computation of the SALI are (1, 1, 1, 1) and (1, 2, 1, 2). In both cases the SALI is the parallel alignment index d_-. The SALI of the ordered orbit G (dashed curve) stabilizes near a non-zero value after a transient time of about 10^4 iterations. The SALI of the chaotic orbit H (solid curve) has a different behaviour almost from the beginning. In particular, it fluctuates a lot, without tending to stabilize around any value and after about 2×10^6 iterations it starts decreasing. The decrease becomes more abrupt after about 10^7 iterations, reaching values of SALI $\approx 10^{-10}$ after 3×10^7 iterations, which means that the two deviation vectors practically coincide.

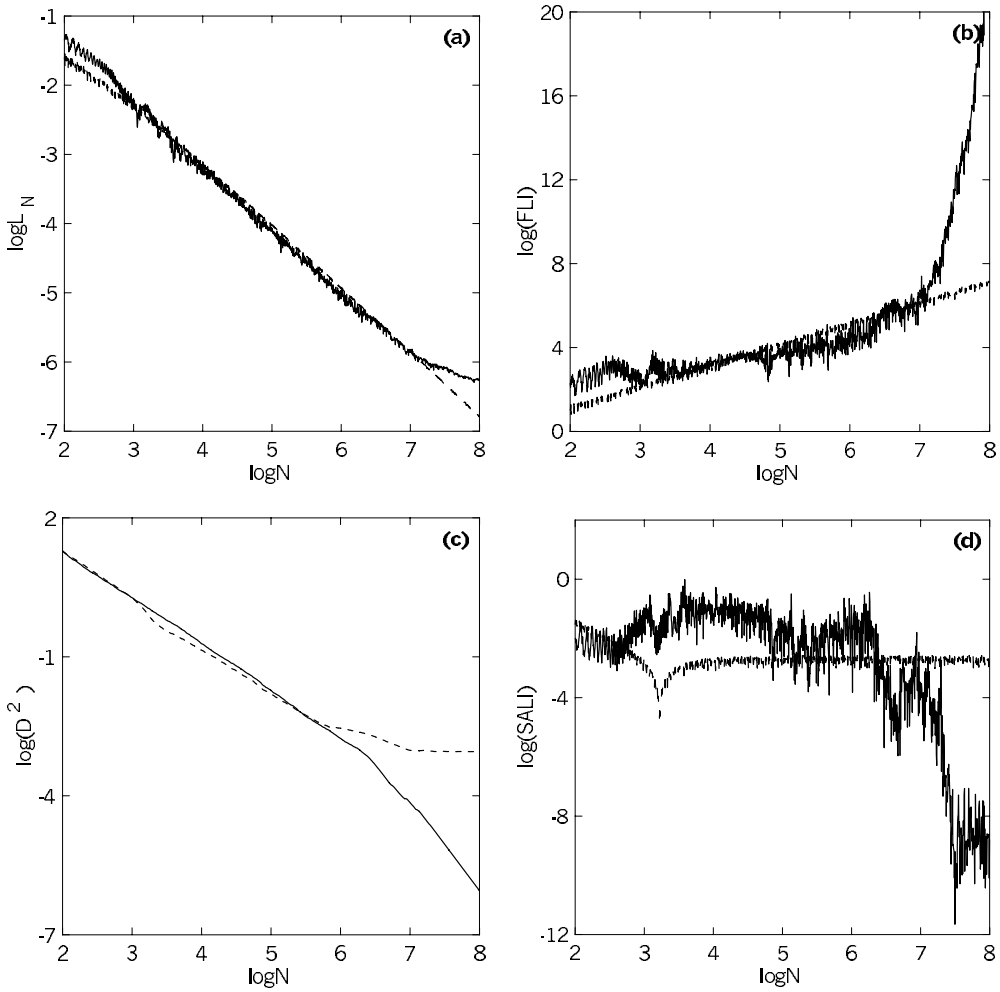

Figure 8. The evolution of (*a*) L_N, (*b*) FLI, (*c*) D^2 and (*d*) SALI, with respect to the number N of iterations of the 4D map (11) with $K = 3$, for the orbits with initial conditions $x_1 = 0.55$, $x_2 = 0.1$, $x_3 = 0.62$, $x_4 = 0.2$ for $\beta = 0.1$ (ordered orbit G, dashed curve) and $\beta = 0.3051$ (slightly chaotic orbit H, solid curve).

Thus, the SALI gives an indication of the chaotic nature of orbit H earlier than any other method used, i.e. after about 2×10^6 iterations. After about 3×10^7 iterations it has very small values, so that the chaotic behaviour of the orbit is established beyond any doubt.

5. Discussion and conclusions

We introduced a fast, efficient and easy to compute method in order to check if orbits of 2D and multidimensional area-preserving maps are ordered or chaotic: the computation of the alignment indices (ALIs). We follow the evolution in time of an orbit and the deviation vectors $v_1(t)$, $v_2(t)$ produced by two initially different vectors $v_1(0)$, $v_2(0)$. At any time step we compute the parallel and antiparallel alignment index

$$d_- \equiv \|v_1(t) - v_2(t)\| \qquad d_+ \equiv \|v_1(t) + v_2(t)\|$$

respectively. When $d_- \to 0$ the two vectors tend to coincide, while if $d_+ \to 0$ the two vectors tend to become opposite to each other. So, the values of the ALIs have a clear physical meaning since they represent the evolution in time of the two deviation vectors and define their relative position in phase space. In particular, the evolution in time of the smaller alignment index (SALI) reflects the chaotic or ordered nature of the orbit. The proposed method classifies definitely an orbit as ordered or chaotic, even in cases of weak chaos. In general, the SALI of nearby chaotic orbits from the same chaotic region have similar behaviour. The same holds for nearby ordered orbits.

In 2D maps the two deviation vectors tend to coincide or become opposite both for ordered and chaotic orbits, but the SALI tends to zero following completely different time rates. In particular, it decreases as the number N of iterations increases, following a power law for ordered orbits, while it decreases abruptly to very small values for chaotic orbits. This different behaviour helps us distinguish between regular and stochastic orbits.

In 4D maps, and in maps of higher dimensionality, things are even better. The deviation vectors tend to coincide or become opposite for chaotic orbits and so the SALI tends to zero, while in general, they remain different for ordered orbits and the SALI tends to a positive non-zero value. So, we can easily decide if an orbit is ordered or chaotic.

An advantage of using the ALIs is that usually, when the orbit under consideration is chaotic, one of them (and of course the SALI) becomes equal to zero, in the sense that it reaches the limit of the accuracy of the computer. After that time the two vectors are identical (equal or opposite), since their coordinates are represented by the same or opposite numbers in the computer. Thus they have exactly the same evolution in time and cannot be separated. In that case the chaotic nature of the orbit is established beyond any doubt. Even in chaotic cases where the SALI does not reach the accuracy limit of the computer (like the case of weak chaos studied in section 4) its values are very small, indicating that the two deviation vectors practically coincide or are opposite.

We also compared this method with other well-known methods that try to determine the ordered or chaotic nature of orbits, in simple cases of regular or stochastic orbits and in a case of weak chaos.

In all cases of 2D, 4D and 6D maps we studied, the use of the SALI helped us decide if an orbit is ordered or chaotic much faster than the computation of the finite time Lyapunov characteristic number L_N.

For orbits in 2D maps the SALI and the FLI have similar behaviour for ordered and chaotic orbits, i.e. the SALI tends to zero, while the FLI tends to infinity in both cases, but both quantities follow different time rates that help us decide if an order is ordered or chaotic. In 4D maps (and in maps of higher dimensionality) the SALI distinguish between ordered and chaotic motion more clearly than the FLI, since the SALI tends to zero for chaotic orbits and to a non-zero value for ordered orbits, while the FLI tends to infinity in both cases (but with different time rates). In general using the SALI we can decide if an orbit is ordered or chaotic at least as fast as by using the FLI.

Finally, we compared the SALI with the spectral distance D of the spectra of stretching numbers produced by two deviation vectors. The computation of the SALI is easier since it is done by simply finding the norms of two vectors, namely $\|v_1(t) - v_2(t)\|$, $\|v_1(t) + v_2(t)\|$ and marking the smaller of these two norms, without having to go through the computation of the spectra of stretching numbers. Another advantage of the SALI is that it can be used for distinguishing between ordered and chaotic orbits even for 2D maps, while the spectral distance D cannot be used in this case. This is due to the fact that in 2D maps the spectra of stretching numbers are invariant to the choice of the initial deviation vectors both for ordered and chaotic orbits.

The spectra of stretching numbers and their spectral distance D exhibit a delay in feeling the changes of the deviation vectors, since they remember the whole evolution in time of the deviation vectors. For instance, although the two deviation vectors may become identical (equal or opposite), their spectra are still different because of the transient phase where the deviation vectors were different. So the SALI determines if an orbit is ordered or chaotic faster than the spectral distance D.

In the present paper we applied different numerical tests in order to distinguish between ordered and chaotic motion in symplectic maps. Our results have the standard accuracy one can achieve with the current computational facilities available. In the examined cases the numerical accuracy we reach and the fact that all numerical tests agree about the chaotic or ordered nature of the orbits, strongly indicate that our results are not spurious.

Acknowledgments

The author would like to thank Professor G Contopoulos and Professor N Voglis for fruitful discussions and also the anonymous referees for several comments which greatly improved the clarity of the paper. This research was supported by the European Union in the framework of $E\Pi ET$ and $K\Pi\Sigma$ 1994–1999 and by the Research Committee of the Academy of Athens.

References

[1] Laskar J 1990 *Icarus* **88** 257
[2] Laskar J 1999 *Hamiltonian Systems with Three or More Degrees of Freedom* ed C Simó (New York: Plenum) p 134
[3] Laskar J, Froeschlé C and Celletti A 1992 *Physica* D **56** 253
[4] Papaphilippou Y and Laskar J 1996 *Astron. Astrophys.* **307** 427
[5] Papaphilippou Y and Laskar J 1998 *Astron. Astrophys.* **329** 451
[6] Froeschlé C, Froeschlé Ch and Lohinger E 1993 *Celest. Mech. Dyn. Astron.* **56** 307
[7] Lohinger E, Froeschlé C and Dvorak R 1993 *Celest. Mech. Dyn. Astron.* **56** 315
[8] Voglis N and Contopoulos G 1994 *J. Phys. A: Math. Gen.* **27** 4899
[9] Contopoulos G, Grousousakou E and Voglis N 1995 *Astron. Astrophys.* **304** 374
[10] Patsis P A, Efthymiopoulos C, Contopoulos G and Voglis N 1997 *Astron. Astrophys.* **326** 493
[11] Contopoulos G and Voglis N 1996 *Celest. Mech. Dyn. Astron.* **64** 1
[12] Contopoulos G and Voglis N 1997 *Astron. Astrophys.* **317** 73
[13] Froeschlé C and Lega E 1998 *Astron. Astrophys.* **334** 355
[14] Voglis N, Contopoulos G and Efthymiopoylos C 1999 *Celest. Mech. Dyn. Astron.* **73** 211
[15] Froeschlé C, Lega E and Gonczi R 1997 *Celest. Mech. Dyn. Astron.* **67** 41
[16] Froeschlé C, Gonczi R and Lega E 1997 *Planet. Space Sci.* **45** 881
[17] Voglis N, Contopoulos G and Efthymiopoylos C 1998 *Phys. Rev.* E **57** 372
[18] Froeschlé C 1972 *Astron. Astrophys.* **16** 172
[19] Contopoulos G and Giorgilli A 1988 *Meccanica* **23** 19
[20] Skokos Ch, Contopoulos G and Polymilis C 1997 *Celest. Mech. Dyn. Astron.* **65** 223
[21] Kantz H and Grassberger P 1988 *J. Phys. A: Math. Gen.* **21** L127